Optimization of Machining Parameters for Product Quality and Productivity in CNC Machining of Aluminium Alloy

Armansyah[*]*, Siti Rohana Nasution, Naufal Dary Dewanto*
Faculty of Engineering, Universitas Pembangunan Nasional Veteran, Jl. RS. Fatmawati Raya, Pd. Labu, 12450 Jakarta, INDONESIA
[*]*armansyah@upnvj.ac.id*

Agus Sudianto
Mechanical Engineering Department, STT YBS Internasional, Jln. Pasar Wetan, Kompleks Mayasari Plasa, 46123 Kota Tasikmalaya, West Java, INDONESIA

Juri Saedon, Shahriman Adenan
College of Engineering, Universiti Teknologi MARA, Shah Alam, Selangor, MALAYSIA

ABSTRACT

This study focused on optimizing the process of CNC machining to enhance productivity and product quality of surface finish R_a via the process parameters of the cutting speed (v_c), feed rate (v_f), and cutting depth (d_{oc}). Experimentation was performed on workpieces of AA-6061 to investigate the response R_a through variation of the process parameters to analyze their best fit using RSM with 2^3 full factorial designs L-8 of DOE. The analysis of variance (ANOVA) was then used to find the major contributors among them that were responsible for the R_a. Based on the result, better R_a was obtained at 0.103 μm using the best fit of v_f (150 mm/min), v_c (220 m/min), and d_{oc} (0.1 mm). ANOVA shows v_f contributed better R_a followed by v_c and d_{oc} respectively. In addition, the level of R_a's was analyzed through contour plots represented by different colours. It continued to analyze the effect of the process parameters via the main effects plot, Pareto chart, and the contour plot in the predictive desirability model, which indicated that the plots and chart confirmed the v_f had more influence compared to others. The study

ISSN 1823-5514, eISSN 2550-164X
Received for review: 2023-11-03
Accepted for publication: 2024-03-31
Published: 2024-09-15

https://doi.org/10.24191/jmeche.v21i3.27351

confirmed that the low-level parameters provided better R_a to be used for polishing.

Keywords: *Conventional CNC Machining; Surface Roughness; Aluminium Alloy; Response Surface Method; Analysis of Variance*

Introduction

The modern manufacturing technology of Industry 5.0 demands resource-efficient, reliable, and sustainable manufacturing processes. One of the common and frequent applications in manufacturing processes is cutting. The cutting performance plays an important role in the quality of the surface finish of the industrial product, particularly its physical and mechanical characteristics. Aluminium alloys including Aluminium metal matrix composite (AMMC) possess a wide range of excellent material properties that make them highly valuable and versatile in various industries. Some of the key properties of Aluminium alloys include lightweight, non-magnetic, corrosion resistant, machinability, recyclability, good electrical and thermal conductivity, as well as good fatigue endurance especially in a high dynamic load [1]-[3], which are suitably used for high precision machining [4]-[6]. Due to these favourable material properties, Aluminium alloys are widely used in various industries, including aerospace, automotive, construction, packaging, consumer electronics, and many more. Engineers and designers often choose Aluminium alloys for their products to take advantage of these unique characteristics and achieve optimal performance and efficiency. However, it can be difficult to work with especially when cut or machined due to having a relatively low melting temperature that often fuses to the cutting edge due to the heat of friction.

The application of computer numerical control machines in CNC machining is a proposed solution to improve productivity and enhance the quality of manufacturing products. The use of CNC machines equipped with advanced control systems to perform machining operations at the specific speed of cuts needs selecting and setting proper machining parameters [7]-[8]. It is aimed to enable faster material removal which in turn reduces cycle times of productivity, and improved surface finish, where it can achieve better surface finishes due to reduced tool chatter and improved cutting dynamics. Other benefits are extended tool life where wear spreads over a longer portion of the flute [9], enhanced precision, and reduced production costs. This involves selecting the appropriate cutting parameters such as cutting speed (v_c), feed rate (v_f), deep of cut (d_{oc}), and tooling material. Proper selection and setting of these parameters are essential to ensure efficient material removal while maintaining the desired product quality.

The surface roughness value (R_a) is one of the essential factors in assessing the effectiveness of the cutting process via uniformity and accuracy of the selected parameters which in turn influences the quality of the surface finish [10]-[11]. Theoretically, surface roughness refers to the unevenness or irregularity of the surface of an object at a level of micro or nanoscale. It is a measure of the small-scale variations in height on a surface, affected by various factors such as manufacturing processes, wear and tear, material properties, and environmental conditions [12]. In fact, surface roughness can significantly affect the performance and functionality of various products and systems. For instance, in engineering applications, a smoother surface is often desirable to reduce friction, wear, and fatigue, while certain processes may require a specific level of roughness for optimal adhesion or lubrication [3]. The roughness of a surface is typically quantified by parameters that characterize the height variations, such as R_a where the absolute values of the roughness profile (arithmetical average roughness), and R_z represents the distance between the highest peak and the lowest valley within a given sampling length (mean peak-to-valley height) [13].

Optimizing the surface roughness during machining involves finding the right balance between the main common parameters applied. The influence of these main parameters such as v_c, d_{oc}, and v_f on the R_a is essential to understanding to optimize the machining process. Each of these parameters plays a significant role in determining the quality of the machined surface. Manufacturers and machinists often conduct experimental studies or use simulation software to determine the optimal cutting conditions for a specific material and machining operation. A study by Bhushan et al. [14], attempted to investigate the influence of v_c, v_f, and d_{oc} on R_a during the machining of 7075 Al alloy and 10 wt.% SiC particulate metal-matrix composites using CNC Turning Machine using tungsten carbide and polycrystalline diamond (PCD) tools. It was found that using the tungsten carbide tool yielded lower R_a affected by a feed range of about 0.1 mm/rev to 0.3 mm/rev and d_{oc} range of about 0.5 mm to 1.5 mm. By using the PCD tool the lower R_a was obtained influenced by a cutting speed of about 220 m/min. Another study by Toan et al. [15], which investigated the effect of machining parameters that consisted of v_c, v_f, and d_{oc} on the R_a in dry-turning Ti6Al4V alloy, stated that v_f is the dominant factor affecting surface roughness, followed v_c and d_{oc}. It was revealed that the R_a was reduced by using the lower v_f, and d_{oc}, and using the higher v_c.

A study by Wang et al. [16] revealed that three machining ranges composed of conventional machining, higher v_c, and ultra-high-speed machining, influenced outcomes via v_c, and d_{oc} on-chip morphology. For instance, CNC milling is running in the range of high speeds, with the consequence that the v_c is selected between 5 to 10 times its conventional v_c. Another study involving v_c, v_f, d_{oc}, and helix angle experimentally on C45 carbon steel was used in optimizing the R_a via regression using ANOVA to

improve the product quality in the surface finish process [17]. An investigation was done by Zhang et al. [18], using the finite element method which influences the residual stress and stress field in Aluminium alloy. This decreased the magnitude of residual stresses in all directions through the increasing v_c. Especially in the aviation area, an efficient approach to Aluminium alloy employing lower stiffness in the thin-walled components. A study done by Zhang et. al. [19], investigated thin-walled AA7075 parts, which demonstrated reduced surface roughness values via optimization of process parameters during machining.

According to the previous studies, it is confirmed that the proper process parameters impacted the quality of the product via evaluation of the surface finish (roughness) R_a on the respected materials. It means that investigation to find the best fit of the process parameter's set was needed in order to optimize the machining process. This can be done through analysis of the proposed values of the process parameters installed, and it became the objective of this study. This study presented optimization of the following key process parameters i.e., v_c, v_f, and d_{oc} using CNC machining through a theoretical model and experimental analysis to assess the R_a of the finished surface on the Al 6061 workpiece. Experimental works on sample specimens are performed using proposed sets of process parameters to obtain data to be used in the analysis study. In the analysis some methods such as RSM and ANOVA were employed, to strengthen the evidence by studying the data. In the end, the characteristics of each process parameter involved during the process were well known, and then a recommendation for the proper set of process parameters that impacted the good R_a can be confirmed. The study roadmap can be seen in Figure 1, explaining that the optimum parameters which feed to CNC machine create a proper and robust machining process via a combination between main parameters of v_c, v_f, and d_{oc} through a theoretical model and experimental analysis in order to obtain high quality of parts to roughness and texture.

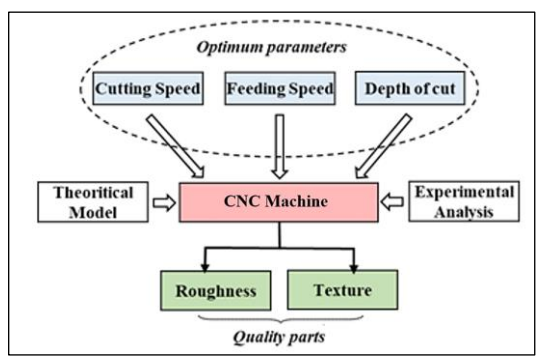

Figure 1: Research outline of surface roughness during CNC machining

Material and Method

In this study Aluminium alloy (AA6061) was used as the workpiece in the experimental analysis due to its lightweight and corrosion-resistant material. The mechanical properties of AA6061 are tabulated in Table 1.

Table 1: Mechanical properties of A 6061 [20]

Properties	Metric	Imperial
Tensile strength	310 MPa	45000 psi
Yield strength	276 MPa	40000 psi
Shear strength	207 MPa	30000 psi
Fatigue strength	96.5 MPa	14000 psi
Elastic modulus	68.9 GPa	10000 ksi
Poisson's ratio	0.33	0.33
Elongation	12-17%	12-17%
Hardness, Brinell	95	95

The raw AA6061 material was produced to become a workpiece with the size of 50 x 38 x 20 mm as shown in Figure 2(a). Experiments are done on the prepared workpiece AA6061 using the Hartford LG-1000 CNC machine available in the lab of Material Engineering and Advanced Manufacturing, at the Engineering Faculty of UPN Veteran Jakarta as in Figure 2(b).

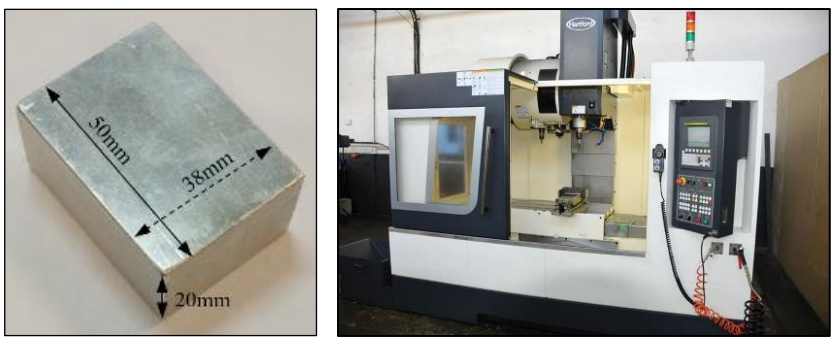

(a) (b)

Figure 2: (a) Completed sample specimen of AA6061 for the experiment, (b) the Hartford LG-1000 of CNC machine

The machining process involved three machining parameters of v_c, v_f, and d_{oc} determined beforehand under low and high levels (Table 2) using an end mill cutter HPMT S42 1000 072, AL SE STD, Ø10 and can be utilized in dry cutting conditions (without coolant).

Table 2: The 3 factors at 2 levels configurations as the low and high level of parameter configurations

Process parameters	Level		Units
	Low	High	
Speed of cut (v_c)	200	220	m/min [21]
Feeding speed (v_f)	150	1681	mm/min
Cutting depth (d_{oc})	0.1	0.5	mm

The next step was planning the experiment using the design of the experiment (DOE) using 2^3 factorial designs L-8 with the response surface method (RSM). These techniques are statistical techniques to optimize the process, improve product quality, and understand the relationship between variables. The DOE plans, conducts, and analyses experiments to know how different factors or variables affect a particular outcome or response of interest with the main objective to efficiently gather information and identify the most critical factors that influence the response. RSM is a technique used in conjunction with DOE to optimize complex processes and find the optimal settings of multiple input variables (factors) that yield better outcomes of response. RSM involves fitting a mathematical model, often a second-order polynomial, to the experimental data obtained from DOE. The DOE of 2^3 factorial designs with the RSM was referred to the full factorial L-8 as the design matrix of central composite (CCD), adopted to form the corner points/vertices, from experiments 1 to 8, of the CCD cube as depicted in Figure 3, and with the factorial design matrix L-8 as tabulated in Table 3. Those number of experiments were repeatedly performed three times for each parameter configuration on the workpiece to overcome the average value of experiment results. The detailed 8 experiments with parameter configurations tabulated in Table 3 were served by the design experts.

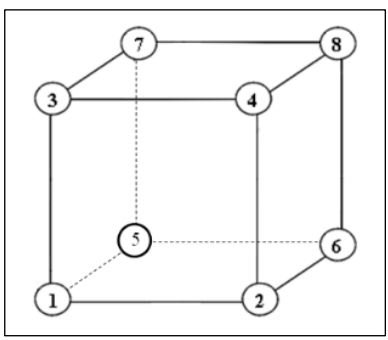

Figure 3: Geometric view of 3 factors with 2 levels of Full Factorial Experimental Design-L8

Table 3: Eight experiments which consist of eight variations of process parameters

Exp.	v_c (m/min)	v_f (mm/min)	d_{oc} (mm)
1	220	150	0.5
2	220	1681	0.5
3	220	150	0.1
4	220	1681	0.1
5	200	150	0.1
6	200	150	0.5
7	200	1681	0.1
8	200	1681	0.5

The response surface method (RSM) was employed for optimizing the significant variables based on data from simulation, and experiments of physical. The dependent factor (*y*) and the independent set variables as input parameters were related by the RSM-based mathematical model. It could be shown as:

$$y = \beta_o + \beta_1 x_1 + \beta_2 + \cdots + \beta_k + \epsilon \quad (1)$$

where y reflects the R_a. A second-order term of the surface texture was RSM-based on the mathematical model where *y* reflecting the approximated value of R_a, is expressed as follows:

$$y = \beta_o + \sum_{i=1}^{k} \beta_i x_i + \sum_{i=1}^{k} \beta_{ii} {x_i}^2 + \sum \sum_{i<j}^{\sim} \beta_{ij} x_i x_i + \epsilon \quad (2)$$

Equation (3) yielded by Design expert using Box-Behnken RSM based on a linear regression model for prediction of the response variable v_c, v_f, and d_{oc} with coefficient factors of v_c, v_f, and d_{oc} [22]. To assess the relative impact of each factor it is common to standardize the coefficient, that involves dividing each coefficient by the standard deviation of the corresponding factor.

$$R_a = \beta_0 + \beta_{v_c} \times \frac{v_c - \bar{v}_c}{SD_{v_c}} + \beta_{v_f} \times \frac{v_f - \bar{v}_f}{SD_{v_f}} + \beta_{d_{oc}} \times \frac{v_{d_{oc}} - \bar{v}_{d_{oc}}}{SD_{d_{oc}}} \quad (3)$$

where:

- $\bar{v}_c, \bar{v}_f,$ and $\bar{v}_{d_{oc}}$: mean values of v_c, v_f, and d_{oc}, respectively;
- $SD_{v_c}, SD_{v_f},$ and $SD_{d_{oc}}$: standard deviation of v_c, v_f, and d_{oc}, respectively;
- β_0 , β_{v_c}, β_{v_f} , and $\beta_{d_{oc}}$: standardized coefficient.

Equation (4) that was obtained by the linear regression model for R_a was found to have 90% accuracy. The final equation in terms in terms of actual factors:

$$R_a = -2.24489 + (0.010637 * v_c) + \left(0.000373 * v_f\right) + (0.353274 * d_{oc}) \quad (4)$$

The share band produces the best R_a. It existed due to the final process. This area denoted a process boundary between the last process and unprocessed material which can be seen in factor 2 (v_f) and factor 3 (d_{oc}) in Table 4.

The R_a results denoted a section of the surface that completed machining. Figure 4 describes the illustration of the workpiece during the milling process with 0.1 mm to 0.5 mm of d_{oc}. The cutting tool is held stationary on the milling machine in a rotary motion, while the table or fixture to bring workpieces moves horizontally to cut the workpiece. The cutting tool is attached to a spindle that rotates at high speed, and the workpiece is fed into the rotating tool to remove material and create the desired shape. The controlling axis in a milling machine refers to the directions in which the workpiece can move. In a typical 3-axis milling machine, the table can move in the X, Y, and Z directions. In this study, the cutting tool removed material from the surface of the workpieces to create a flat, smooth surface through facing operation, via a rotated tool cut in the CNC milling machine. The CNC milling machine table moved in the horizontal direction from the first point of cut at the edge of the workpiece and ended at the other edge of the workpiece. Then, the cutting tool does the same action for the next round of the milling process in the opposite direction which is so called the zigzag path of the cutting tool.

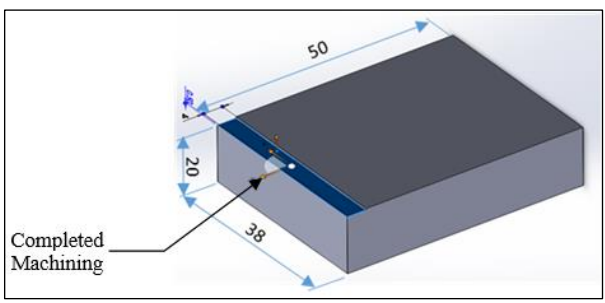

Figure 4: Workpiece after the machining process

After machining, the finished cutting of the sample specimen was measured at three different locations randomly located on the workpiece

surface along the cutting path using a surface roughness tester of Surfcoder SE300 (Figure 5) as an output response R_a from the CNC machining processes. The measurement was done by attaching the sensor from the measuring tool of the surface roughness tester to the point at 3 different locations on the workpiece randomly along the cutting path. Finally, the study continued by data analysis using ANOVA, to explore the significant contribution of machining parameters influencing R_a. The result obtained from the experiment and analysis will be then concluded and documented.

Figure 5: Surface roughness tester of Surfcoder SE300

Results and Discussion

The R_a's values from experiments 1 to 8 are shown in Table 4. It can be seen that the response of R_a of each run provided different results where the lowest R_a (0.103 µm) was achieved at the third run by using v_c (220 m/min), v_f (150 mm/min), and doc (0.1 mm). The highest R_a was obtained at 0.975 µm, at the second run, where v_c (220 m/min), v_f (1681 mm/min), and d_{oc} (0.5 mm) were set. Table 4 shows that good R_a could be reached by using a low level of machining parameters.

Table 4: Design layout

Run	Factor 1	Factor 2	Factor 3	Response
	A: v_c (m/min)	**B: v_f (mm/min)**	**C: d_{oc} (mm)**	**mean R_a**
1	220	150	0.5	0.216
2	220	1681	0.5	0.975
3	220	150	0.1	0.103
4	220	1681	0.1	0.876
5	200	150	0.1	0.123
6	200	150	0.5	0.161
7	200	1681	0.1	0.360
8	200	1681	0.5	0.676

The result obtained from the response surface linear model via Analysis of variance (ANOVA) can be shown in Table 5. The F-value of 10.59, which was the ratio of explained variance to unexplained variance via the calculation of two mean squares, explained that this model was very noteworthy. The mean squares of 2.26% possibility indicated that this F-value happened due to noise. Subsequently, the P-values (0.0226) that were less than 0.05, denoted the model's term was substantial, which meant the model was important. Values with more than 0.10 indicated that the model's terms were not significant [23]. If there are many insignificant model terms, the reduction of the model could be possibly improved.

Table 5: Analysis of variance (ANOVA) for response surface linear model

Source	**Sum of square**	**df**	**Mean square**	**F-Value**	**p-value Prob > F**	**Remark**
Model	0.7825	3	0.2608	10.59	0.0226	significant
v_c	0.0905	1	0.0905	3.67	0.1277	
v_f	0.6520	1	0.6520	26.47	0.0068	
d_{oc}	0.0399	1	0.0399	1.62	0.2719	
Residual	0.0985	4	0.0246			
Cor Total	0.8810	7				

Table 6 presented the predicted at 0.553 as R^2 was not as close to the adjusted R^2 at 0.804 as normally expected. It was different from more than 0.2. This declared a large block effect or a potential problem with the model of data. All of the empirical models should be tested by doing confirmation experiments. The precision model measured the signal-to-noise ratio, where a ratio of more than 4 was desirable. The ratio of 8.335 denoted an adequate signal. Therefore, this model could be employed to serve the design space [24].

Table 6: Fit of statistics

Standard deviation	**0.157**
Mean	0.436
C.V.%	35.98
R^2	0.888
Adjusted R^2	0.804
Predicted R^2	0.553
Adeq precision	8.335

Table 7 shows the overall average of all expected changes in the factor values when the remaining factors are constant. This was represented by the estimated average adjustment based on factor settings. When the VIFs were 1, the factors were orthogonal, so that the VIFs greater than 1. It indicated the

VIF was higher. It meant the correlation of factors was more severe. A rough rule standard revealed that a VIF less than 10 was tolerable [25].

Table 7: Coded factors coefficients

Factors	Coefficient estimate	df	Error of standard	95% low of CI	95% high of CI	VIF
Intercept	-0.0956	1	0.2830	-0.8812	0.6901	
A-v_c	0.6832	1	0.3330	-0.2862	1.56	1.0000
B-v_f	0.2855	1	0.0555	0.1314	0.4396	1.0000
C-d_{oc}	0.0707	1	0.0555	-0.0834	0.2247	1.0000

Figure 6 shows the main effect plot via Minitab for R_a in accordance with the impact of v_c, v_f, and d_{oc}. It can be seen that v_f had the steepest slope and longest line which possessed respective factors of high effect on the R_a which confirmed having a significant effect on the surface finish response R_a compared to the other two parameters of v_c and d_{oc} [26], due to the v_f mainly affected by the interaction between the cutting tool and the workpiece material. The higher v_f typically results in a larger volume of material being removed per unit of time. However, need to balance the v_f with other cutting parameters such as v_c and d_{oc} to achieve optimal surface finish and minimize surface roughness R_a. It was also shown that faster v_c produced smaller R_a values and vice versa. The main effect plot for R_a confirmed that the most suitable process parameter was at 150 mm/min of v_f, 220 m/min of v_c, and 0.1 mm of d_{oc}.

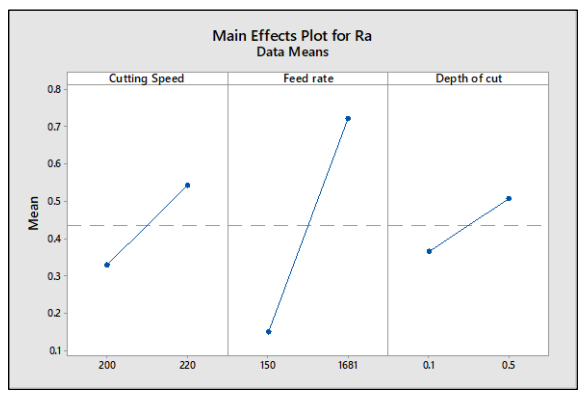

Figure 6: The main effects plot for R_a

Figure 7 depicts the Pareto chart ordered with the bars indicating the highest frequency of occurrence to the lowest frequency of occurrence. It shows evidence that v_f reached the standardized effect of about 0.58 (58%) through the screening test, while v_c of about 0.22 (22%) and d_{oc} of about others

0.15 (15%). This confirmed that the v_f contributed the highest parameter contribution to the output response of surface roughness value R_a, followed by v_c and d_{oc}, respectively.

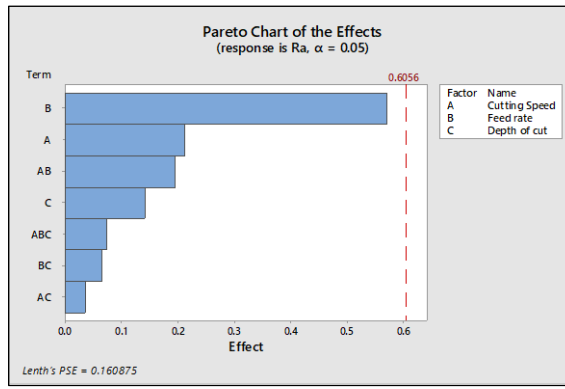

Figure 7: The pareto chart of the effect

Figure 8 presents a graphical representation of the relationship between predicted and actual results. This linear regression model denoted the contribution of machining parameters within creating a equation linear to build a linear graph of graphical representation of the relationship between predicted and actual results. This linear regression model denoted the contribution of machining parameters within creating a equation linear to build a linear graph [27]. Multiple machining parameters and more complex linear regression models can be used to predict the response variable accurately. The graph helps visualize how well the model captures the linear relationship between the predictors and the response. The fitted line will be a straight line that best fits the data points, showing the linear relationship between the predicted and actual values. In the plot, each data point represents an actual result (Z) corresponding to specific values of machining parameters. The fitted line goes through the data points to best approximate the linear relationship between the Z and the machining parameters. Ideally, in a perfect linear relationship, all data points would fall exactly on the fitted line. However, in real-world scenarios, there may be some variation, and the goal of the linear regression model is to minimize the difference between the predicted values (on the fitted line) and the actual data points.

The actual test results obtained with the linear regression model in Figure 8 and the estimated values are compared in R^2 of 0.888 taken from Table 6. The values of the outcome experiment results were revealed to each contour of the selected result.

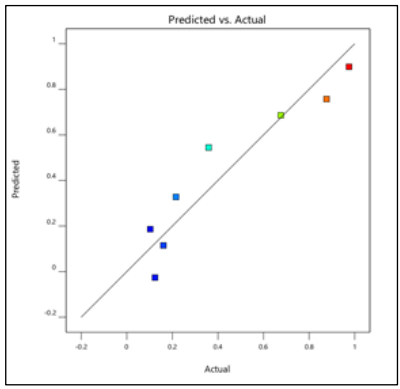

Figure 8: Comparison of the linear regression model with experimental results

In Figure 9(a), a contour plot for desirability visualized the combined performance of multiple response variables such as v_c and v_f into a single desirability value. The plot had two machining parameters i.e., v_c and v_f, and the desirability values represented by contour with colours. In this plot, different regions were highlighted based on the desirability level. Higher desirability regions had desirability 1 which is in the red colours region, indicating areas where the machining parameters result in more desirable outcomes. Lower desirability regions will have contour colour more widely spaced, indicating regions where the performance is less desirable [28].

A contour plot for R_a, as depicted in Figure 9(b), visualized the relationship between v_c and v_f to the R_a of completed machining on sample specimens. The plot had a v_c on the X-axis and a v_f on the Y-axis, and the contour plot represented by colour indicated different levels of R_a. Regions with smoother surfaces had a colour plot of blue colour, indicating lower R_a values, while regions with rougher surfaces had a colour plot of green to yellow colour, indicating higher R_a values. The selected predicted value came up from Figure 5(b) was 0.09390 μm.

A contour plot for the standard error of design, Figure 9(c), involved varying different design parameters and evaluated the impact on the standard error of a given response variable. The plot shows how the standard error of the response variable varied across the design space, allowing to identify a region with lower or higher uncertainty in the model prediction. Each contour in the plot represented a specific value of the standard error, and the shape and orientation of the contour hung on the distribution of data [29]. In the plot can be seen around 205 to 212 m/min of v_c represented lower errors about 0.4 m/min. The standard error changed across the design space and identified regions with higher or lower errors in the model predictions.

In Figure 9(d), an overlay plot represented the combination of two or more response variables as a contour plot on the same graph. It allowed to visualize how different factors affected multiple responses simultaneously, and provided valuable insights into the relationships between the factors and responses. By looking at the intersection of the contour lines, it could be observed how the responses changed in relation to each other based on varying design factors, to identify regions in the design space, where both responses were desirable, or where one response might improve at the expense of the other [30]. The plot can be used to confirm the optimization process, it could assess the impact of the design factors on multiple responses visually and simultaneously. The plot shows the predicted R_a at 0.065 µm by the v_c at 190.81 m/min and v_f of 390.52 mm/min as shown in Figure 7(d). The selected value was close to the desirability 1 as denoted in Figures 9(a) and 9(b).

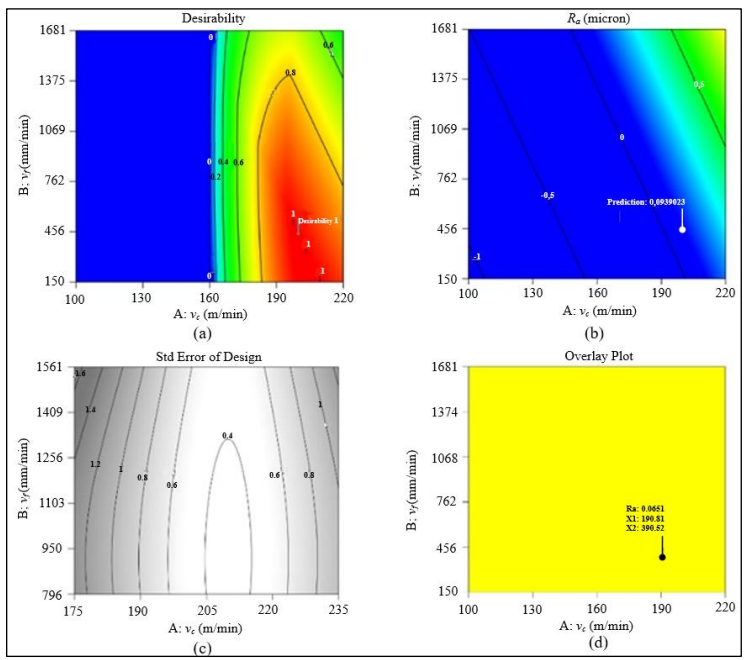

Figure 9: (a) is a contour plot for desirability, under v_c versus v_f, (b) is a contour plot for R_a, under v_c versus v_f, (c) is a contour plot for standard error of design, under v_c versus v_f, and (d) is a contour plot for overlay plot, under v_c versus v_f

Based on the experiment, desires for the optimal values of the three input parameters are identified. Figure 10 represents a 3D surface plot to

visualize the relationship between machining parameters in optimization and analysis at low-level machining parameters. The plot was managed at varied v_c and v_f with the constant d_{oc} to the response of R_a. It can be seen that the 3D surface plot shows the response R_a was varied between ±1 as v_c and v_f were varied. The dark blue colour region was dominated by lower v_c and v_f which was indicated by the lower R_a. On the other hand, the green to orange colour regions were dominated by higher v_c and v_f which was indicated by the higher R_a. This fulfilled the statement that the lower R_a could be reached by low-level machining parameters. However, the good R_a could be seen between 0.1 µm - 0.5 µm which covered the bright blue regions, by setting the v_f and v_c between 150 mm/min - 1681 mm/min and 160 m/min - 210 m/min, respectively were kept constant at their middle level.

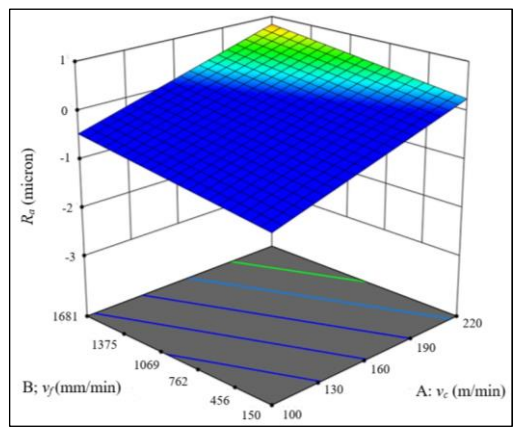

Figure 10: Model graph-3D surface

Figure 11 shows, images of the surface roughness textures on the finished machining of the sample specimen in macroscopic. Figure 11(a) presents an image of surface roughness in the middle of the back cut, which refers to the quality of the machined or cut surface on the backside of a workpiece, on a scale of 0.2 mm with the mean value R_a about 0.221 µm. Figure 11(b) depicts an image of surface roughness in the middle of smearing with the mean value R_a of 0.162 µm affected by the heat and pressure due to machining yielding deformation of metal along the edges of a cut on a scale of 1.0 mm. Smearing typically refers to the process of spreading or smudging a material over a surface which can impact the surface finish influenced by factors like tool geometry, cutting conditions, or lubrications. Close to the shear band, which was a localized strain in a narrow zone of intense shearing strain, an image of homogenous deformation from machining indicated a good result of surface roughness [31]. Figure 11(c) shows an image of the best

surface roughness on the side of the smearing on a scale of 0.2 mm with the mean value R_a near to 0.103 μm.

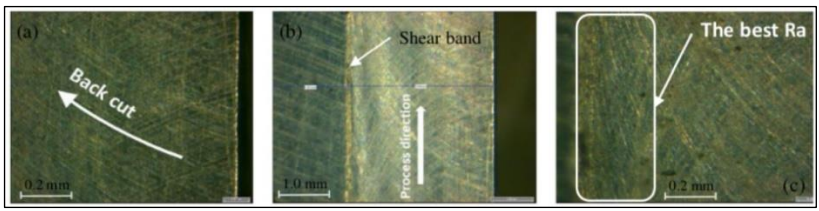

(a) (b) (c)

Figure 11: Macroscopic analysis on surface texture of finished machining AA6061 and roughness profile in 0.2 mm scales, in (a) roughness in the middle back cut process, (b) roughness in the middle smearing process, and (c) in the side smearing process

Conclusion

This study investigated the response R_a through experiments on workpiece of AA6061 using CNC machining, which was influenced by process parameters of v_c, v_f, and d_{oc} via DOE using RSM. ANOVA was also then used to analyze the experimental data of RSM and DOE. Based on the results, better R_a could be reached at 0.103 μm with the best fit of machining parameters of v_f (150 mm/min), v_c (220 m/min), and d_{oc} (0.1 mm). ANOVA found that v_f provided the most significant parameters in CNC Machining on AA6061 with a p-value of 0.0068 and the mean squares of 2.26% possibility which indicated this F-value happened due to noise. The main effects plot shows that v_f yields a major effect on R_a. In addition to the prediction model, it was revealed that the ratio of 8.335 denoted an adequate signal measured the signal-to-noise ratio, where a ratio of more than 4 was desirable. Therefore, this model could be employed to serve the design space. Furthermore, contour plots were presented to confirm the proposed process parameter via predicted R_a at 0.065 μm using v_c and v_f at 190.81 m/min and 390.52 mm/min respectively where the selected value was close to the desirability. Subsequently, a 3D surface plot visualized the relationship between machining parameters where the lower R_a could be reached by low-level machining parameters with low v_c and low v_f. Confirmation was also made via macroscopic analysis on the images of the finish machining of the sample specimen where homogenous deformation from machining indicated a good result of surface roughness R_a. It can be concluded that the proposed process parameters are suitable for polishing purposes.

Contributions of Authors

The authors confirm the equal contribution in each part of this work. All authors reviewed and approved the final version of this work.

Funding

This work was supported by the "HIBAH INTERNAL PENELITIAN UPN VETERAN JAKARTA RISCOP 2022" [719/UN61.0/HK.02/2022].

Conflict of Interests

The authors confirm the equal contribution in each part of this work. All authors reviewed and approved the final version of this work.

Acknowledgment

The authors especially would like to thank the Engineering Faculty and LPPM of the Universitas Pembangunan Nasional "Veteran", Jakarta, Indonesia, for the internal research grant scheme of RISCOP 2022 awarded, College of Engineering, Universiti Teknologi MARA, Shah Alam, Selangor, Malaysia, and STT YBS Internasional Tasikmalaya, West Java Indonesia, for the support given in the collaboration.

References

[1] N. H. Alharthi, S. Bingol, A. T. Abbas, A. E. Ragab, E. A. El-Danaf, and H. F. Alharbi, "Optimizing cutting conditions and prediction of surface roughness in face milling of az61 using regression analysis and artificial neural network", *Advances in Materials Science and Engineering*, vol. 2017, pp. 1–8, 2017. doi: 10.1155/2017/7560468

[2] D. Raabe, D. Ponge, P. J. Uggowitzer, "Making sustainable aluminum by recycling scrap: The science of 'dirty' alloys", *Progress in Materials Science*, vol. 128, pp. 1-150, 2022. doi: 10.1016/j.pmatsci.2022.100947

[3] Z. Wang, R. Ye, and J. Xiang, "The performance of textured surface in friction reducing: A review", *Tribology International*, vol. 177, pp. 1-12, 2023. doi: 10.1016/j.triboint.2022.108010

[4] M. Aamir, M. Tolouei-Rad, K. Giasin, A. Vafadar, U. Koklu, and W. Keeble, "Evaluation of the surface defects and dimensional tolerances in

multi-hole drilling of AA5083, AA6061, and AA2024", *Applied Sciences*, vol. 11, no. 9, pp. 1-15, 2021. doi: 10.3390/app11094285

[5] M. Ş. Adin, "Performances of cryo-treated and untreated cutting tools in machining of AA7075 aerospace aluminium alloy", *European Mechanical Science*, vol. 7, no. 2, pp. 70–81, 2023. doi: 10.26701/ems.1270937

[6] D. E. Sander, H. Allmaier, H. H. Priebsch, F. M. Reich, M. Wiitt, A. Skiadas, and O. Knaus, "Edge loading and running-in wear in dynamically loaded journal bearings," *Tribology International*, vol. 92, pp. 395–403, 2015. doi: 10.1016/j.triboint.2015.07.022

[7] K. A. Al-Ghamdi and A. Iqbal, "A sustainability comparison between conventional and high-speed machining," *Journal of Cleaner Production*, vol. 108, pp. 192–206, 2015. doi: 10.1016/j.jclepro.2015.05.132

[8] K. H. Hashmi, G. Zakria, M. B. Raza, and S. Khalil, "Optimization of Process Parameters for High Speed machining of Ti-6Al-4V using response surface methodology," *The International Journal of Advanced Manufacturing Technology*, vol. 85, no. 5–8, pp. 1847–1856, 2016. doi: 10.1007/s00170-015-8057-3

[9] Eldar Gerfanov, "Resources and Software For High-Performance CNC Machinists: Numbers Behind High Speed Machining (HSM)," May 28, 2013. [Online]. Available: https://zero-divide.net/?article_id=4413_numbers-behind-high-speed-machining-hsm.

[10] I. Maher, M. E. H. Eltaib, A. A. D. Sarhan, and R. M. El-Zahry, "Investigation of the effect of machining parameters on the surface quality of machined brass (60/40) in CNC end milling—ANFIS modeling," *The International Journal of Advanced Manufacturing Technology*, vol. 74, no. 1–4, pp. 531–537, 2014. doi: 10.1007/s00170-014-6016-z

[11] C. Shanshan, C. C. Fai, Z. Feihu, H. L. Ting, and Z. Chenyang, "Theoretical and experimental investigation of a tool path control strategy for uniform surface generation in ultra-precision grinding," *The International Journal of Advanced Manufacturing Technology*, vol. 103, no. 9–12, pp. 4307–4315, 2019. doi: 10.1007/s00170-019-03852-6

[12] Y. Gong, J. Xu, and R. C. Buchanan, "Surface roughness: A review of its measurement at micro-/nano-scale", *Physical Sciences Reviews*, vol. 3, no. 1, 2018. doi: 10.1515/psr-2017-0057

[13] Bharat Bhushan, "Surface Roughness Analysis and Measurement Techniques," in *Modern Tribology Handbook*, 1st ed., vol. 1, Bharat Bhushan, Ed., Ohio: CRC Press, 2000, pp. 49–114.

[14] R. K. Bhushan, S. Kumar, and S. Das, "Effect of machining parameters on surface roughness and tool wear for 7075 Al alloy SiC composite,"

The International Journal of Advanced Manufacturing Technology, vol. 50, no. 5–8, pp. 459–469, 2010. doi: 10.1007/s00170-010-2529-2

[15] N. Van Toan, N. Thi Hai Van, N. Kim Hung, and D. Tat Khoa, "Prediction of surface roughness of Ti6Al4V and optimization of cutting parameters based on experimental design," *Journal of Military Science and Technology*, vol. 87, pp. 108–116, 2023. doi: 10.54939/1859-1043.j.mst.87.2023.108-116

[16] B. Wang, Z. Liu, Q. Song, Y. Wan, and Z. Shi, "Proper selection of cutting parameters and cutting tool angle to lower the specific cutting energy during high speed machining of 7050-t7451 aluminum alloy," *Journal of Cleaner Production*, vol. 129, pp. 292–304, 2016. doi: 10.1016/j.jclepro.2016.04.071

[17] N.-T. Nguyen, "A study on influence of milling types and cutting conditions on surface roughness in milling of aluminum alloy Al6061-T6," *Universal Journal of Mechanical Engineering*, vol. 8, no. 4, pp. 183–190, 2020. doi: 10.13189/ujme.2020.080403

[18] W. Zhang, S. Li, Q. Wu, and Z. An, "Study on finite element method of stress field in aluminum alloy high-speed milling process," *IOP Conference Series Materials Science and Engineering*, vol. 269, pp. 1-7, 2017. doi: 10.1088/1757-899X/269/1/012088

[19] X. Zhang, J. wei Ma, Z. yuan Jia, and D. ning Song, "Machining parameter optimisation for aviation aluminium-alloy thin-walled parts in high-speed milling," *International Journal of Machining and Machinability of Materials*, vol. 20, no. 2, p. 180, 2018. doi: 10.1504/ijmmm.2018.090546

[20] T. Hong, F. Ding, F. Chen, H. Zhang, Q. Zeng, and J. Wang, "Mechanical properties of 6061 aluminum alloy under cyclic tensile loading," *Crystals (Basel)*, vol. 13, no. 8, p. 1171, 2023. doi: 10.3390/cryst13081171

[21] A. Sudianto, Z. Jamaludin, A. A. Abdul Rahman, S. Novianto, and F. Muharrom, "Automatic temperature measurement and monitoring system for milling process of aa6041 aluminum aloy using mlx90614 infrared thermometer sensor with arduino," *Journal of Advanced Research in Fluid Mechanics and Thermal Sciences*, vol. 82, no. 2, pp. 1–14, 2021. doi: 10.37934/arfmts.82.2.114

[22] A. Nooraziah and V. J. Tiagrajah, "A study on regression model using response surface methodology," *Applied Mechanics and Materials*, vol. 666, pp. 235–239, 2014. doi: 10.4028/www.scientific.net/AMM.666.235

[23] Robert Odek and Gordon Opuodho, "F-test and P-values: A synopsis," *Journal of Management and Science*, vol. 13, no. 2, pp. 59–61, 2023. doi: 10.26524/jms.13.22

[24] A. Y. Aminy, A. Hayat, and M. Mudassir, "The influence of machining variables on the quality of the shaping process on hard steel," *Key Engineering Materials*, vol. 948, no. 1, pp. 41–47, 2023. doi: 10.4028/p-8z5yoa

[25] J. Ferré, "Regression diagnostics," in *Comprehensive Chemometrics*, vol. 3, pp. 33–89, 2009. doi: 10.1016/B978-044452701-1.00076-4

[26] R. D., V. S. Mudakappanavar, T. K. Chavan, and R. Suresh, "Effect of process parameters on surface roughness, thrust force and tool wear of coated hss tool during drilling of customized EN8 alloy," *Journal of Mechanical Engineering*, vol. 19, no. 3, pp. 113–134, 2022. doi: 10.24191/jmeche.v19i3.19799

[27] S. Winarni, N. Sunengsih, and I. Ginanjar, "Multi responses Taguchi optimization using overlaid contour plot and desirability function," *Journal of Physics: Conference Series*, vol. 1776, no. 1, pp. 1-9, 2021. doi: 10.1088/1742-6596/1776/1/012061

[28] V. K. Sharma, M. Rana, T. Singh, A. K. Singh, and K. Chattopadhyay, "Multi-response optimization of process parameters using desirability function analysis during machining of EN31 steel under different machining environments," *Materials Today: Proceedings*, vol. 44, pp. 3121–3126, 202,. doi: 10.1016/j.matpr.2021.02.809

[29] Q.-B. Xiao, M. Wan, W.-H. Zhang, and Y. Yang, "Tool orientation optimization for the five-axis CNC machining to constrain the contour errors without interference," *Journal of Manufacturing Processes*, vol. 76, pp. 46–56, 2022. doi: 10.1016/j.jmapro.2022.01.071

[30] W. Ming. Y. Zhang, X. Li, D. Shen. W. He, J. Ma, and F. Shen, "Multi-objective optimization based IBCS for surface roughness and textural feature in MCVE piston machining," *The International Journal of Advanced Manufacturing Technology*, vol. 97, no. 1–4, pp. 1285–1304, 201. doi: 10.1007/s00170-018-1989-7

[31] Pro-lean, "*Surface Roughness: Everything You Need to Know*," Dec 23, 2022. [Online]. Available: https://proleantech.com/surface-roughness-everything-you-need-to know/#:~:text=Polished%3A%20Ra%200.05%2D0.2%20%C2%B5m,texture%20for%20bonding%20or%20painting.